Preprints of the 21st IFAC World Congress (Virtual)
Berlin, Germany, July 12-17, 2020

A Semi-global Hybrid Sensorless Observer for Permanent Magnet Synchronous Machines with Unknown Mechanical Model

Alessandro Bosso * **Ilario A. Azzollini** * **Andrea Tilli** *

* *Department of Electrical, Electronic and Information Engineering, University of Bologna, Bologna, Italy (e-mail: {alessandro.bosso3, ilario.azzollini, andrea.tilli}@unibo.it).*

Abstract: In this paper, we present a hybrid sensorless observer for Permanent Magnet Synchronous Machines, with no a priori knowledge of the mechanical dynamics and without the typical assumption of constant or slowly-varying speed. Instead, we impose the rotor speed to have a constant (unknown) sign and a non-zero magnitude at all times. For the design of the proposed scheme, we adopt meaningful Lie group formalism to describe the rotor position as an element of the unit circle. This choice, however, leads to a non-contractible state space, and therefore it introduces topological constraints that complicate the achievement of global/semi-global and robust results. In this respect, we show that the proposed observer, which augments a recent continuous-time solution, achieves semi-global practical asymptotic stability by periodically resetting the estimates. As highlighted in the simulation results, the novel hybrid strategy leads to improved transient performance, notably without any modification of the gains employed in the continuous-time version. These features motivate to augment the observer with a discrete-time identifier, leading to significantly faster rotor flux reconstruction.

Keywords: Nonlinear Observers and Filter Design; Stability of Hybrid Systems; Lyapunov Methods; Input-to-State Stability

1. INTRODUCTION

Permanent Magnet Synchronous Machines (PMSMs) are nowadays widely adopted in several fields, ranging from vehicle propulsion to industrial motion applications. In many contexts, rotor position and speed are required to achieve accurate regulation, yet the presence of mechanical sensors may pose reliability and economic issues. Furthermore, such sensors often result impractical because of space and weight requirements, e.g., in small/medium size electrically-powered Unmanned Aerial Vehicles (UAVs). In this respect, the so-called sensorless control techniques aim to replace mechanical sensors with suitable reconstruction algorithms and have been the subject of extensive research efforts. Several design strategies from nonlinear control theory have been applied to sensorless control. To name a few, we recall Extended Kalman Filters (Hilairet et al., 2009), Sliding Mode (Lee and Lee, 2013) and High Gain and Adaptive strategies (Montanari et al., 2006; Marino et al., 2008; Khalil et al., 2009). Recently, some works have been dedicated to Interior Permanent Magnet Synchronous Machines (Ortega et al., 2019) and stator resistance estimation (Verrelli et al., 2017) (see also Verrelli et al. (2018) for a solution with available rotor speed).

In the field of sensorless control and observation, the capability of dealing with highly variable speed, with little to no a priori knowledge of the mechanical dynamics, becomes crucial to achieve high-end, high precision algorithms when motors are coupled with nonlinear time-varying loads. This is the case e.g. for the electric propulsion of UAVs or Hybrid Electric Vehicles (HEVs), where the environmental conditions heavily affect the external torque. In this context, the recent works (Bobtsov et al., 2015; Bernard and Praly, 2018) propose observers able to reconstruct the rotor position and flux, independently of the mechanical model. In (Tilli et al., 2019), a sixth-order observer with unknown mechanical model is developed employing a unit circle representation for the rotor angular configuration, and in (Bosso et al., 2020) such design is conveniently exploited for torque control and resistance estimation. Indeed, the unit circle (indicated with $\mathbb{S}^1$) is a compact abelian Lie group, and Lyapunov-based tools can be used to derive a simple stability analysis. Specifically, the algorithm in (Tilli et al., 2019) exploits a high gain observer to reconstruct the back-Electromotive Force (back-EMF), which is then used to set up an adaptive attitude estimator on $\mathbb{S}^1$. The resulting reduced-order dynamics, corresponding to the attitude observer reconstruction error, is shown to evolve on the cylinder $\mathbb{S}^1 \times \mathbb{R}$.

The use of a compact Lie group representation, however, introduces some relevant challenges. In fact, it is known that when a dynamical system evolves on a manifold that is not diffeomorphic to any Euclidean space, it is impossible for a continuous vector field to globally asymptotically stabilize an equilibrium point (Mayhew et al., 2011). This phenomenon arises in (Tilli et al., 2019) since two isolated hyperbolic equilibria are present, a stable node/focus and a saddle point: this restricts the basin of attraction of the reduced-order dynamics to $(\mathbb{S}^1 \times \mathbb{R}) \backslash \mathcal{R}_{\mathcal{U}}$, where $\mathcal{R}_{\mathcal{U}}$ is a curve passing through the saddle equilibrium. This property directly affects the full-order observer and only regional stability can be established. We report the observers on $SO(3)$ studied in (Mahony et al., 2008), which display a similar behavior in a higher dimensional context. Notably, an attempt to break this kind of topological constraints with discontinuous and memoryless feedback leads to non-robust solutions, induc-

ing in practice chattering behaviors. Indeed, a dynamic hybrid feedback law must be employed in order to achieve global *and* robust results (Sontag, 1999; Mayhew et al., 2011).
In this work, we introduce a hybrid modification to the position, speed and flux observer of (Tilli et al., 2019) intending to establish semi-global instead of regional stability. An alternative to the continuous-time strategy is possible because both components of the back-EMF vector are available as indirect measurement, thus allowing to detect when the angular estimation error settles to a wrong configuration. Exploiting this fact, we introduce a simple strategy based on a clock to periodically reset the position reconstruction. The rotor speed is restricted to have a constant (unknown) sign and to be bounded in norm from above and below by positive scalars. These conditions are compatible with many applications, including the control of propeller motors, where the sign of speed is usually not reversed. The properties of the observer are highlighted through two time scales arguments (see e.g. (Teel et al., 2003; Sanfelice and Teel, 2011)), and numerically compared to the structure in (Tilli et al., 2019). In particular, we underline the interesting feature that, if the same tuning gains are adopted for the observer flows, the new algorithm displays a consistently faster transient response. Finally, inspired by these enhanced convergence properties, we also propose an augmentation based on a discrete-time identifier to further boost the estimation performance, at the expense of increased computational complexity.
The structure of the paper is the following. After a brief introduction to the mathematical background in Section 2, we formally state the observer problem in Section 3. The observer structure is presented in Section 4, while in Section 5 we outline some concluding remarks and future research directions.

2. NOTATION

We use $(\cdot)^T$ to denote the transpose of real-valued matrices. For simplicity we often indicate with (v, w), for a pair of column vectors v, w, the concatenated vector $(v^T, w^T)^T$. In case of non-differentiable signals, the upper right Dini derivative, indicated with D^+, is employed as generalized derivative.

2.1 The Unit Circle Formalism

We employ the unit circle $\mathbb{S}^1$ to represent reference frames involved in the manipulation of PMSM equations, as in (Tilli et al., 2019). In particular, $\mathbb{S}^1$ is a compact abelian Lie group, with the planar 2-D rotation employed as group operation. An integrator on $\mathbb{S}^1$ is given by

$$\dot{\zeta} = u(t)\mathcal{J}\zeta, \quad \mathcal{J} = \begin{pmatrix} 0 & -1 \\ 1 & 0 \end{pmatrix}, \quad \zeta \in \mathbb{S}^1,$$

with $u(t) \in \mathbb{R}$. Any angle $\vartheta \in \mathbb{R}$ can be mapped into an element of $\mathbb{S}^1$ given by $(\cos(\vartheta)\ \sin(\vartheta))^T$. Finally, to any $\zeta = (c\ s)^T \in \mathbb{S}^1$ we can associate a rotation matrix $\mathcal{C}[\zeta] = \begin{pmatrix} c & -s \\ s & c \end{pmatrix}$, used for group multiplication: for any $\zeta_1, \zeta_2 \in \mathbb{S}^1$, the product is given by $\zeta_1 \cdot \zeta_2 = \mathcal{C}[\zeta_1]\zeta_2 = \mathcal{C}[\zeta_2]\zeta_1$, with identity element $(1\ 0)^T$.

2.2 Hybrid Dynamical Systems

In this paper we adopt the formalism of hybrid dynamical systems as in (Goebel et al., 2012). In particular, a hybrid system $\mathcal{H}$ can be described as

$$\mathcal{H} : \begin{cases} \dot{x} & \in F(x,u) \qquad (x,u) \in C \\ x^+ & \in G(x,u) \qquad (x,u) \in D \end{cases}$$

where x is the state, u is the input, C is the flow set, F is the flow map, D is the jump set, and G is the jump map. The state of the hybrid system can either flow according to the differential inclusion $\dot{x} \in F$ (while $(x,u) \in C$), or jump according to the difference inclusion $x^+ \in G$ (while $(x,u) \in D$). For the main concepts related to hybrid solutions, stability, robustness, and related Lyapunov theory, we refer to (Goebel et al., 2012) and references therein.

3. MODEL FORMULATION AND PROBLEM STATEMENT

The electromagnetic model of a PMSM in a static bi-phase reference frame, under balanced working conditions, linear magnetic circuits and negligible iron losses, can be written as

$$\frac{d}{dt} i_s = -\frac{R}{L} i_s + \frac{1}{L} u_s - \frac{\omega \varphi \mathcal{J} \zeta}{L}, \qquad \dot{\zeta} = \omega \mathcal{J} \zeta, \tag{1}$$

where $i_s, u_s \in \mathbb{R}^2$ are the stator currents and voltages, respectively. In particular, u_s is a piecewise continuous and locally essentially bounded signal defined over $[t_0, \infty)$, with initial time t_0. Furthermore, ω is the electrical angular speed, while $\zeta \in \mathbb{S}^1$ and $\varphi \in \mathbb{R}_{>0}$ are the angular configuration and the constant amplitude of the rotor magnetic flux vector, respectively. Finally, R is the stator resistance and L is the stator inductance. In the field of sinusoidal machines, it is common to represent (1) in rotating reference frames. Consider a generic frame with orientation $\zeta_r \in \mathbb{S}^1$ and speed ω_r. Then, (1) becomes

$$\begin{aligned} \frac{d}{dt} i_r &= -\frac{R}{L} i_r + \frac{1}{L} u_r - \frac{\omega \varphi \mathcal{J} \mathcal{C}^T[\zeta_r]\zeta}{L} - \omega_r \mathcal{J} i_r \\ \dot{\zeta} &= \omega \mathcal{J} \zeta, \qquad \dot{\zeta}_r = \omega_r \mathcal{J} \zeta_r, \end{aligned} \tag{2}$$

where $i_r = \mathcal{C}^T[\zeta_r] i_s$, $u_r = \mathcal{C}^T[\zeta_r] u_s$. In this work, ω is modeled as an unknown bounded input, subject to the following regularity assumption.

Assumption 1. The signal $\omega(\cdot)$ is defined over the interval $[t_0, \infty)$ and, in addition:

- $\omega(\cdot)$ is $\mathcal{C}^0$ and piecewise $\mathcal{C}^1$ in its domain of existence;
- there exist positive scalars $\omega_{\min}$, $\omega_{\max}$ such that, for all $t \geq t_0$, it holds $\omega_{\min} \leq |\omega(t)| \leq \omega_{\max}$;
- $|D^+\omega(t)|$ exists and is bounded, for all $t \geq t_0$.

Note that these conditions ensure existence and uniqueness of solutions on $[t_0, \infty)$. Additionally, since the properties that we specified for the input signals do not depend on t_0, we can choose $t_0 = 0$ without loss of generality. Assumption 1 requires the angular speed ω to have constant sign and uniformly non-zero magnitude. This condition is slightly more restrictive than the well-known assumption of non-permanent zero speed, which was proven to be a sufficient condition to reconstruct ω, ζ, and φ, assuming currents and voltages available for measurement and the parameters R and L perfectly known (Zaltni et al., 2010). Nevertheless, Assumption 1 is compatible with significant applications such as renewables electric energy generation and electric vehicles propulsion (UAVs, HEVs).
We finally recall the problem of *sensorless observer, with (restricted) variable speed and no mechanical model* (Tilli et al., 2019): given the PMSM model (1) or (2), design an estimator of ζ, ω, φ with only stator voltages and currents available for measurement, such that appropriate stability and convergence properties hold under Assumption 1.

Table 1. System and observer parameters

Stator resistance R [Ω]	0.06	k_p	2.18×10^4
Stator inductance L [μH]	33.75	k_i	9.34×10^3
Nominal angular speed [rpm]	6000	k_η	95.7
Rotor magnetic flux φ [mWb]	1.9	γ	4582
Number of pole pairs p	7	Λ	200
Load Inertia [Kgm^2]	2.5×10^{-5}	N	2

4. THE PROPOSED HYBRID OBSERVER

In this section we present the main result of this work, and we compare it with a preliminary continuous-time solution. To simplify the presentation and highlight the connection between the different strategies, we embed along the text some numerical results, based on a UAV propeller motor, whose parameters are indicated in Table 1. Since the observer transient performance is more evident when it is disconnected from the controller, we employ a standard sensorized field-oriented controller to generate the speed profile ω. We omit the complete closed-loop simulations for brevity.

4.1 The χ-Reference Frame and a Continuous-Time Solution

Let $\chi := |\omega|\varphi \in \mathbb{R}_{>0}$, $\xi := (1/\varphi)\operatorname{sgn}(\omega)$. This allows to replace the PMSM angular dynamics considering the particular frame $\zeta_\chi := \zeta \operatorname{sgn}(\xi) = \zeta \operatorname{sgn}(\omega)$, which yields a simple reformulation of the model, for a generic rotating frame ζ_r:

$$\begin{aligned} \frac{d}{dt} i_r &= -\frac{R}{L} i_r + \frac{1}{L} u_r - \frac{\chi \mathcal{J} \mathcal{C}^T[\zeta_r]\zeta_\chi}{L} - \omega_r \mathcal{J} i_r \\ \dot{\zeta}_\chi &= \chi \xi \mathcal{J} \zeta_\chi, \qquad \dot{\zeta}_r = \omega_r \mathcal{J} \zeta_r. \end{aligned} \tag{3}$$

Note that $\xi \in \mathbb{R}$ is an unknown parameter, while χ satisfies the following properties, as a direct consequence of Assumption 1:

- χ is $\mathcal{C}^0$ and piecewise $\mathcal{C}^1$;
- $\chi_\mathrm{m} \leq \chi \leq \chi_\mathrm{M}$, for some positive scalars χ_m, χ_M;
- $|D^+\chi| \leq M$, for some positive scalar M.

The main idea of the proposed observer is to design an estimator of ζ_χ employing as representation the frame $\zeta_r = \hat{\zeta}_\chi$, whose dynamics is designed so that the two references synchronize asymptotically. This synchronization problem can be recast as the stabilization of the misalignment error $\eta := \mathcal{C}^T[\hat{\zeta}_\chi]\zeta_\chi \in \mathbb{S}^1$. For convenience, let the subscript $(\cdot)_{\hat{\chi}}$ indicate the electric variables in the frame $\hat{\zeta}_\chi$, leading to:

$$\begin{aligned} \frac{d}{dt} i_{\hat{\chi}} &= -\frac{R}{L} i_{\hat{\chi}} + \frac{1}{L} u_{\hat{\chi}} - \frac{\chi \mathcal{J} \eta}{L} - \hat{\omega}_\chi \mathcal{J} i_{\hat{\chi}} \\ \dot{\zeta}_\chi &= \chi \xi \mathcal{J} \zeta_\chi, \qquad \dot{\hat{\zeta}}_\chi = \hat{\omega}_\chi \mathcal{J} \hat{\zeta}_\chi, \end{aligned} \tag{4}$$

with $\hat{\omega}_\chi$ the angular speed of the frame $\hat{\zeta}_\chi$. In (Tilli et al., 2019), the synchronization problem was addressed with a continuous-time observer of the form

$$\begin{aligned} \dot{\hat{\imath}} &= -\frac{R}{L}\hat{\imath} + \frac{1}{L} u_{\hat{\chi}} + \frac{\hat{h}}{L} - \left(|\hat{h}|\hat{\xi} + k_\eta \hat{h}_1\right) \mathcal{J} i_{\hat{\chi}} + k_\mathrm{p} \tilde{\imath} \\ \dot{\hat{h}} &= k_\mathrm{i} \tilde{\imath} \qquad \dot{\hat{\zeta}}_\chi = \left(|\hat{h}|\hat{\xi} + k_\eta \hat{h}_1\right) \mathcal{J} \hat{\zeta}_\chi \qquad \dot{\hat{\xi}} = \gamma \hat{h}_1 \end{aligned} \tag{5}$$

where $\hat{\imath}$ is the estimated current ($\tilde{\imath} := i_{\hat{\chi}} - \hat{\imath}$), $\hat{\xi}$ and $\hat{h}$ are the estimates of ξ and the back-EMF $h = -\chi \mathcal{J} \eta$, respectively, while the angular speed is $\hat{\omega}_\chi = |\hat{h}|\hat{\xi} + k_\eta \hat{h}_1$. Finally, k_p, k_i, k_η and γ are positive scalars, whereas the observer outputs are given by $\hat{\omega} = |\hat{h}|\hat{\xi}$, $\hat{\zeta} = \hat{\zeta}_\chi \operatorname{sgn}(\hat{\xi})$ and $\hat{\varphi} = \operatorname{sat}(1/|\hat{\xi}|)$, where the bounds of the saturation are chosen according to the motor parameter ranges.

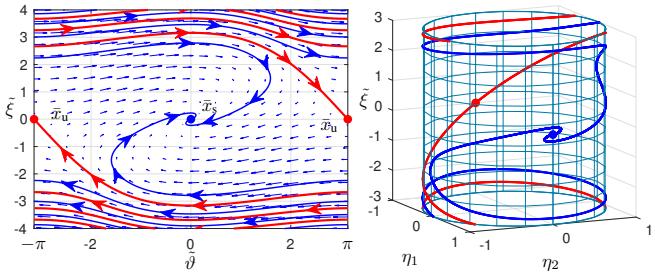

Fig. 1. Phase diagram of (6) for $\chi = 1$, $k_\eta = 1.5$, $\gamma = 1$ as in (Tilli et al., 2019). *Left*: the unstable manifold (red) and some trajectories converging to $\bar{x}_\mathrm{s}$ (blue), depicted on the planar representation $(\tilde{\vartheta}, \tilde{\xi})$, where $\tilde{\vartheta} = \operatorname{atan2}(\eta_2, \eta_1)$ is the angle in the interval $[-\pi; \pi)$ corresponding to η. *Right*: the same objects represented on the cylinder $\mathbb{S}^1 \times \mathbb{R}$.

In (Tilli et al., 2019), it was proven that regional practical asymptotic stability is ensured by proper selection of k_p and k_i. This stems from the two time scales approach used to separate the dynamics into a fast subsystem, given by a high-gain observer for current and back-EMF estimation, and a slow subsystem, an adaptive attitude observer on $\mathbb{S}^1$. From the slow subsystem derives the inherently regional and not semi-global result: the reduced order error dynamics, obtained under perfect knowledge of $i_{\hat{\chi}}$ and h, is written on the cylinder $\mathbb{S}^1 \times \mathbb{R}$ as follows ($\tilde{\xi} := \xi - \hat{\xi}$):

$$\dot{\eta} = \left(\chi \tilde{\xi} - k_\eta \chi \eta_2\right) \mathcal{J} \eta \qquad \dot{\tilde{\xi}} = -\gamma \chi \eta_2. \tag{6}$$

Indeed, the domain of attraction of the configuration $\bar{x}_\mathrm{s} = ((1,0),0) \in \mathbb{S}^1 \times \mathbb{R}$, corresponding to rotation alignment and correct flux estimation, does not include an unstable manifold of dimension 1 (shown in Figure 1), originating from the saddle equilibrium $\bar{x}_\mathrm{u} = ((-1,0),0)$. Figure 2 (plots (a),(d),(g),(j)) presents the simulation results corresponding to observer (5) with the same gains as in (Tilli et al., 2019). Note that the initial transient (corresponding to high values of $|\tilde{\xi}|$) is relatively slow, highlighting the same helicoidal shape as in Figure 1.

4.2 A Hybrid Strategy for Semi-Global Stability

With the insights provided by the above observer, we modify system (6) enriching its dynamics with a jump policy, while preserving the existent flows. In particular, we propose to augment the observer with a clock, given by:

$$\begin{cases} \dot{\rho} = \Lambda & \rho \in [0,1] \\ \rho^+ = 0 & \rho = 1 \end{cases} \tag{7}$$

with Λ a positive scalar for tuning. The proposed clock can be used to enforce jumps of the angular estimate at regular times and thus break the cylinder topological constraint, but it seems also convenient as a way to embed additional desirable features. Among these, we will propose a simple identifier to enhance the transient performance. To begin, we introduce a baseline strategy with no identifier. In place of (6), consider system:

$$\mathcal{H}_0 : \begin{cases} \begin{pmatrix} \dot{\eta} \\ \dot{\tilde{\xi}} \\ \dot{\rho} \end{pmatrix} = \begin{pmatrix} \left(\chi \tilde{\xi} - k_\eta \chi \eta_2\right) \mathcal{J} \eta \\ -\gamma \chi \eta_2 \\ \Lambda \end{pmatrix} =: F_0 \begin{pmatrix} \eta \\ \tilde{\xi} \\ \rho \end{pmatrix} \in C_\mathrm{s} \\ \begin{pmatrix} \eta^+ \\ \tilde{\xi}^+ \\ \rho^+ \end{pmatrix} \in \begin{pmatrix} \begin{cases} -F\eta, & \chi\eta_1 \leq 0 \\ \eta, & \chi\eta_1 \geq 0 \end{cases} \\ \tilde{\xi} \\ 0 \end{pmatrix} =: G_0 \begin{pmatrix} \eta \\ \tilde{\xi} \\ \rho \end{pmatrix} \in D_\mathrm{s} \end{cases} \tag{8}$$

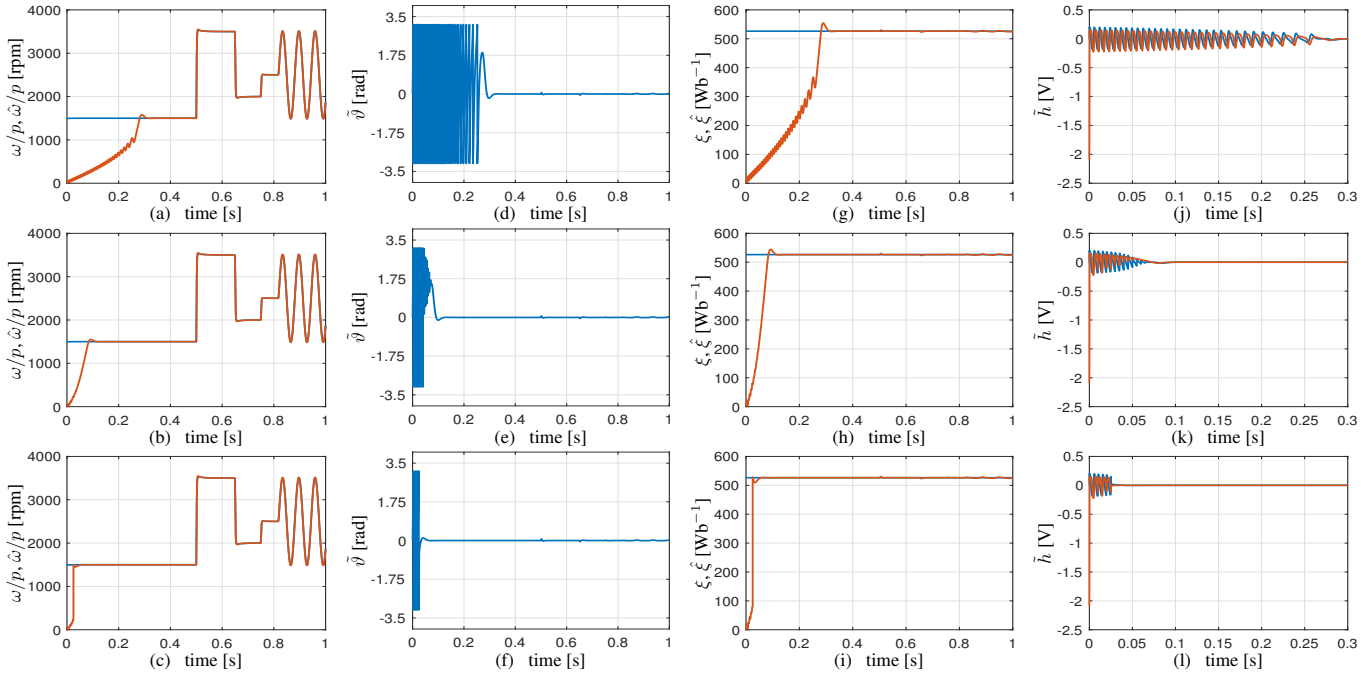

Fig. 2. First row: observer (5). Second row: observer (13). Third row: observer (13)-(22)-(23). (a),(b),(c): Rotor angular speed (blue) and estimated value (red). (d),(e),(f): Rotor angular position reconstruction error. (g),(h),(i): Parameter ξ (blue) and its estimate (red). (j),(k),(l): Back-EMF reconstruction error, with the first component in blue and the second one in red.

where $F = \text{diag}\{1,-1\}$, while $C_\text{s} = \mathbb{S}^1 \times \mathbb{R} \times [0,1]$ and $D_\text{s} = \mathbb{S}^1 \times \mathbb{R} \times \{1\}$. Let $x_\text{s} := (\eta, \tilde{\xi}, \rho) \in \mathbb{S}^1 \times \mathbb{R} \times [0,1]$. In this structure, the angle η is always reset to a value satisfying $\eta_1 \geq 0$, thus ensuring that the set $\bar{x}_\text{u} \times [0,1]$ is not forward invariant. In fact, the next result confirms that the proposed hybrid strategy removes the unstable manifold $\mathcal{R}_\mathcal{U}$.

Lemma 1. The set $\mathcal{A}_0 := \bar{x}_\text{s} \times [0,1] \subset \mathbb{S}^1 \times \mathbb{R}^2$ is a uniformly preasymptotically stable attractor for system $\mathcal{H}_0$, with basin of preattraction given by $\mathbb{S}^1 \times \mathbb{R}^2$.

Proof: It is a direct application of the Nested Matrosov Theorem for hybrid systems (Sanfelice and Teel, 2009, Theorem 4.1). Consider the following Matrosov functions (bounded in any compact set of x_s by Assumption 1):

$$W_1(x_\text{s},\chi) = 1 - \eta_1 + \frac{1}{2\gamma}\tilde{\xi}^2, \quad W_2(x_\text{s},\chi) = -\chi\tilde{\xi}\eta_1\eta_2$$
$$W_3(x_\text{s},\chi) = \exp(\rho)\left[\eta_2^2 + \tilde{\xi}^2\right], \quad W_4(x_\text{s},\chi) = \frac{1-\eta_1}{\exp(\rho)}. \tag{9}$$

It holds $\sup_{f \in F_0(x_\text{s},\chi)} \langle \nabla W_i(x_\text{s},\chi), (f, D^+\chi)\rangle \leq B_{\text{c},i}(x_\text{s})$, $i \in \{1,2,3,4\}$, for all $x_\text{s} \in C_\text{s}$, with bounds given by:

$$B_{\text{c},1} = -k_\eta \chi_\text{m} \eta_2^2 \leq 0, \quad B_{\text{c},2} = -\chi_\text{m}^2 \eta_1^2 \tilde{\xi}^2 + \Delta_2(x_\text{s})|\eta_2|$$
$$B_{\text{c},3} = \Lambda W_3 + \Delta_3(x_\text{s})|\eta_2|, \; B_{\text{c},4} = -\Lambda\frac{1-\eta_1}{\exp(\rho)} + \Delta_4(x_\text{s})|\eta_2|,$$

with Δ_2, Δ_3, Δ_4 positive continuous functions in their arguments. Note that $B_{\text{c},2} \leq -\chi_\text{m}^2\tilde{\xi}^2$ as $\eta_2 = 0$, thus in $B_{\text{c},3}$ and $B_{\text{c},4}$ the conditions 1)-2) of (Sanfelice and Teel, 2009, Theorem 4.1) must be checked in particular for $\eta_1 = -1$, $\eta_2 = 0$, $\tilde{\xi} = 0$, for any $\rho \in [0,1]$. Similarly, it holds $\sup_{g \in G_0(x_\text{s},\chi)} W_i(g,\chi) - W_i(x_\text{s},\chi) \leq B_{\text{d},i}(x_\text{s})$, $i \in \{1,2,3,4\}$, for all $x_\text{s} \in D_\text{s}$, with the following bounds (let $\Delta_g = \exp(1) - \exp(0) > 0$):

$$B_{\text{d},1} = \min\{0, 2\eta_1\} \leq 0, \quad B_{\text{d},2} = \max\{0, -2\chi_\text{M}|\tilde{\xi}||\eta_2|\eta_1\}$$
$$B_{\text{d},3} = -\Delta_g(\eta_2^2 + \tilde{\xi}^2), \quad B_{\text{d},4} = \frac{\Delta_g}{\exp(1)}(1 - |\eta_1|).$$

It can be verified from the first three bounds that the conditions 1)-2) of (Sanfelice and Teel, 2009, Theorem 4.1) are satisfied for all $x_\text{s} \in D_\text{s} \backslash \mathcal{A}_0$. Finally, note that uniform global stability is easily established with $B_{\text{c},1}$, $B_{\text{d},1}$, in connection with the fact that W_1 is positive definite (considering a proper indicator function) with respect to the attractor $\mathcal{A}_0$, for all $x_\text{s} \in C_\text{s} \cup D_\text{s} \cup G_0(D_\text{s})$. Since all sufficient conditions in (Sanfelice and Teel, 2009) are verified, the statement follows immediately. □

To derive the observer structure, we now compute the jumps of $\hat{\zeta}_\chi$ corresponding to $\eta^+ = -F\eta$ using $\hat{h}$ as a proxy of $h = -\chi\mathcal{J}\eta$. For, note that $-F\eta = \mathcal{C}^T[\hat{\zeta}_\chi^+]\zeta_\chi = \mathcal{C}[\zeta_\chi]F\hat{\zeta}_\chi^+$, therefore it is possible to express $\hat{\zeta}_\chi^+$ as:

$$\hat{\zeta}_\chi^+ = -F\mathcal{C}^T[\zeta_\chi]F\eta = -\mathcal{C}[\zeta_\chi]\eta = -\mathcal{C}^T[\hat{\zeta}_\chi][\mathcal{C}[\zeta_\chi]\zeta_\chi]. \tag{10}$$

Furthermore, a "fast" estimate of the rotor position (rescaled by χ) can be retrieved from $\hat{h}$ and $\hat{\zeta}_\chi$, since $\mathcal{J}h = \chi\eta$, and therefore $\chi\zeta_\chi = \mathcal{C}[\hat{\zeta}_\chi]\mathcal{J}h$. These considerations yield $G_\zeta : \mathbb{R}^2 \times \mathbb{S}^1 \rightrightarrows \mathbb{S}^1$:

$$G_\zeta(\hat{h},\hat{\zeta}_\chi) \in \begin{cases} -\mathcal{C}^T[\hat{\zeta}_\chi]\begin{pmatrix}\cos(2\theta_\chi(\hat{h},\hat{\zeta}_\chi))\\ \sin(2\theta_\chi(\hat{h},\hat{\zeta}_\chi))\end{pmatrix}, & \hat{h}_2 \geq 0 \\ \hat{\zeta}_\chi, & \text{otherwise} \end{cases} \tag{11}$$

$$\theta_\chi = \text{atan2}(y_\chi, x_\chi) \subset [-\pi,\pi], \quad (x_\chi \; y_\chi)^T = \mathcal{C}[\hat{\zeta}_\chi]\mathcal{J}\hat{h}$$

where we let $\text{atan2}(0,0) = [-\pi,\pi]$ and $\text{atan2}(y,x) = \{-\pi,\pi\}$, for all (x,y) in the set $S = \{(x,y) \in \mathbb{R}^2 : x < 0, y = 0\}$ [1]. Let $G_\text{f}(\hat{h},\hat{\zeta}_\chi) = \mathcal{C}^T[G_\zeta(\hat{h},\hat{\zeta}_\chi)]\mathcal{C}[\hat{\zeta}_\chi]$ indicate the change of coordinates from the $\hat{\zeta}_\chi$-frame to the $\hat{\zeta}_\chi^+$-frame. This map, available for observer design, is employed to describe the jumps that occur both to $i_{\hat{\chi}}$ and h:

$$i_{\hat{\chi}}^+ = \mathcal{C}^T[\hat{\zeta}_\chi^+]i_s = \mathcal{C}^T[G_\zeta(\hat{h},\hat{\zeta}_\chi)]\mathcal{C}[\hat{\zeta}_\chi]\mathcal{C}^T[\hat{\zeta}_\chi]i_s = G_\text{f} i_{\hat{\chi}}$$
$$h^+ = -\chi\mathcal{J}\mathcal{C}^T[\hat{\zeta}_\chi^+]\zeta_\chi = G_\text{f} h. \tag{12}$$

[1] Clearly, atan2 can be implemented as single-valued in the actual algorithm.

It follows that the overall observer structure is given by:

$$\begin{pmatrix} \dot{\hat{\imath}} \\ \dot{\hat{h}} \\ \dot{\hat{\zeta}}_\chi \\ \dot{\hat{\xi}} \\ \dot{\hat{\rho}} \end{pmatrix} = \begin{pmatrix} -\frac{R}{L}\hat{\imath} + \frac{1}{L}u_{\hat{\chi}} + \frac{\hat{h}}{L} - \hat{\omega}_\chi \mathcal{J} i_{\hat{\chi}} + k_{\mathrm{p}}\tilde{\imath} \\ k_{\mathrm{i}}\tilde{\imath} \\ \hat{\omega}_\chi \mathcal{J}\hat{\zeta}_\chi \\ \gamma \hat{h}_1 \\ \Lambda \end{pmatrix} \quad \rho \in [0,1]$$
$$\begin{pmatrix} \hat{\imath}^+ \\ \hat{h}^+ \\ \hat{\zeta}_\chi^+ \\ \hat{\xi}^+ \\ \rho^+ \end{pmatrix} \in \begin{pmatrix} G_{\mathrm{f}}(\hat{h}, \hat{\zeta}_\chi)\hat{\imath} \\ G_{\mathrm{f}}(\hat{h}, \hat{\zeta}_\chi)\hat{h} \\ G_\zeta(\hat{h}, \hat{\zeta}_\chi) \\ \hat{\xi} \\ 0 \end{pmatrix} \quad \rho = 1 \tag{13}$$

with $\hat{\omega}_\chi = |\hat{h}|\hat{\xi} + k_\eta \hat{h}_1$ as before. Let $x_{\mathrm{f}} := T(\tilde{\imath}, \tilde{h}) \in \mathbb{R}^4$, with $\tilde{h} := h - \hat{h}$ and T a matrix such that (Tilli et al., 2019):

$$x_{\mathrm{f}} = T \begin{pmatrix} \tilde{\imath} \\ \tilde{h} \end{pmatrix} = \begin{pmatrix} \varepsilon^{-1} I_2 & 0_{2\times 2} \\ -\varepsilon^{-1} I_2 & L^{-1} I_2 \end{pmatrix} \begin{pmatrix} \tilde{\imath} \\ \tilde{h} \end{pmatrix}, \tag{14}$$

with ε a positive scalar such that $R/L + k_{\mathrm{p}} = 2\varepsilon^{-1}$, $k_{\mathrm{i}} = 2L\varepsilon^{-2}$. We can define the overall error dynamics as follows:

$$\begin{pmatrix} D^+ x_{\mathrm{f}} \\ \dot{x}_{\mathrm{s}} \end{pmatrix} = \begin{pmatrix} \varepsilon^{-1} \underbrace{\begin{pmatrix} -I_2 & I_2 \\ -I_2 & -I_2 \end{pmatrix}}_{A_{\mathrm{f}}} x_{\mathrm{f}} + \underbrace{\begin{pmatrix} 0_{2\times 2} \\ L^{-1} I_2 \end{pmatrix}}_{B_{\mathrm{f}}} f_h \\ F_{\mathrm{s}}(x_{\mathrm{f}}, \chi, x_{\mathrm{s}}) \end{pmatrix} \quad x_{\mathrm{s}} \in C_{\mathrm{s}}$$
$$\begin{pmatrix} x_{\mathrm{f}}+ \\ x_{\mathrm{s}}^+ \end{pmatrix} \in \begin{pmatrix} \mathrm{diag}\{G_{\mathrm{f}}, G_{\mathrm{f}}\} x_{\mathrm{f}} \\ G_{\mathrm{s}}(x_{\mathrm{f}}, \chi, x_{\mathrm{s}}) \end{pmatrix} \quad x_{\mathrm{s}} \in D_{\mathrm{s}} \tag{15}$$

with $f_h = D^+ h$ defined exactly as in (Tilli et al., 2019), and F_{s}, G_{s} the flows and jumps of the attitude estimation error (which correspond to the data in (8) if $\tilde{h} = 0$), respectively. Note that it holds $A_{\mathrm{f}} + A_{\mathrm{f}}^T = -2I_4$, while the jump x_{f}^+ preserves the norm:

$$\begin{aligned} |x_{\mathrm{f}}^+|^2 &= |\varepsilon^{-1}\tilde{\imath}^+|^2 + |L^{-1}\tilde{h}^+ - \varepsilon^{-1}\tilde{\imath}^+|^2 \\ &= |G_{\mathrm{f}}\varepsilon^{-1}\tilde{\imath}|^2 + |G_{\mathrm{f}}(L^{-1}\tilde{h} - \varepsilon^{-1}\tilde{\imath})|^2 \\ &= |\varepsilon^{-1}\tilde{\imath}|^2 + |L^{-1}\tilde{h} - \varepsilon^{-1}\tilde{\imath}|^2 = |x_{\mathrm{f}}|^2. \end{aligned} \tag{16}$$

This means that on the one hand, during flows, the x_{f}-subsystem can be made arbitrarily fast by choosing ε sufficiently small, while on the other hand the jumps do not cause any increase of $|x_{\mathrm{f}}|$, and thus they do not represent an obstacle to time scale separation. We summarize the stability properties of the above hybrid system in the following theorem, which represents the main result of this work.

Theorem 1. Consider system (15) with inputs $\chi(\cdot)$, $D^+\chi(\cdot)$, satisfying Assumption 1 and let $(\psi_{\mathrm{f}}(\cdot), \psi_{\mathrm{s}}(\cdot))$ indicate its solutions, with initial conditions $(x_{\mathrm{f},0}, x_{\mathrm{s},0})$. Denote with ρ_0 the initial condition of the clock. Then, the attractor $0_{4\times 1} \times \mathcal{A}_0$ is semi-globally practically asymptotically stable as $\varepsilon \to 0^+$, i.e.:

- there exists a proper indicator σ_{s} of $\mathcal{A}_0$ in $\mathbb{S}^1 \times \mathbb{R}^2$;
- there exists a class $\mathcal{KL}$ function β_{s};

such that, for any positive scalars Δ_{f}, Δ_{s}, δ, there exists a scalar $\varepsilon^* > 0$ such that, for all $0 < \varepsilon \le \varepsilon^*$, all $(\psi_{\mathrm{f}}(\cdot), \psi_{\mathrm{s}}(\cdot))$ satifying $\rho_0 = 0$, $|x_{\mathrm{f},0}| \le \Delta_{\mathrm{f}}$ and $\sigma_{\mathrm{s}}(x_{\mathrm{s},0}) \le \Delta_{\mathrm{s}}$, the following bounds hold, for all $(t,j) \in \mathrm{dom}(\psi_{\mathrm{f}}(\cdot), \psi_{\mathrm{s}}(\cdot))$:

$$\begin{aligned} |\psi_{\mathrm{f}}(t,j)| &\le \exp\left(-t/\varepsilon\right) |x_{\mathrm{f},0}| + \delta \\ \sigma_{\mathrm{s}}(\psi_{\mathrm{s}}(t,j)) &\le \beta_{\mathrm{s}}(\sigma_{\mathrm{s}}(x_{\mathrm{s},0}), t+j) + \delta. \end{aligned} \tag{17}$$

Figure 2 (plots (b),(e),(h),(k)) presents the simulation results corresponding to observer (13), with Λ selected as in Table 1. Notably, this new solution enhances the convergence performance of the previous continuous-time algorithm. This is motivated by the intuition that the jumps, for Λ sufficiently large, impose the position estimation error η to be close during transients either to $(0,\ 1)$ or to $(0,\ -1)$: these configurations are associated with the maximal value of $|\dot{\hat{\xi}}|$. For this reason, we can expect that there exists a range for $|\dot{\hat{\xi}}|$ where the convergence properties of this observer are optimized. In particular, this range is expected to be between large errors, where the continuous time angular "wraps" dominate the behavior, and small errors, where jumps do not cause any correction.

4.3 A Mini-Batch Identifier for Enhanced Initial Convergence

We conclude this section with a modification of the above strategy to ensure a faster observer response, obtained by means of a discrete-time identifier. The need to employ a higher number of state variables, in addition to performing the minimization of a cost function, clearly makes this method more computationally intensive. However, some strategies can be adopted to mitigate the online burden and enable implementation in embedded computing systems (e.g., moving the procedure in a lower priority/frequency task).

Firstly, recall that a perturbed estimate of $\chi\zeta_\chi$ can be computed as $\mathcal{C}[\hat{\zeta}_\chi]\mathcal{J}\hat{h}$. From the solutions of system (3) it can be noted that, for any positive scalar T, for all $t \ge T$:

$$\zeta_\chi(t) - \zeta_\chi(t-T) = \xi \mathcal{J} \int_{t-T}^{t} \chi(s)\zeta_\chi(s) ds. \tag{18}$$

Multiplying both sides by $\chi(t-T)\chi(t)$ it follows ($y(s) = \chi(s)\zeta_\chi(s)$):

$$\chi(t-T)y(t) - \chi(t)y(t-T) = \xi\chi(t-T)\chi(t)\mathcal{J}\int_{t-T}^{t} y(s) ds, \tag{19}$$

which can be constructed with division-free estimates, since χ can be replaced with $|\hat{h}|$ and y with $\mathcal{C}[\hat{\zeta}_\chi]\mathcal{J}\hat{h}$. Indeed, between jumps of the clock (7), we can compactly rewrite (19) as $X(t,j) + e_X(t,j) = (\Phi(t,j) + e_\Phi(t,j))\xi$, where X and Φ are only function of $\hat{h}$, $\hat{\zeta}_\chi$, their past values and their integrals, while e_X and e_Φ are disturbances depending on h and $\tilde{h}$. For $N \in \mathbb{N}_{\ge 1}$, let $\tau_N(\cdot)$ be a moving window operator such that, for a hybrid arc ψ satisfying jumps according to the clock (7) (with $\rho(0,0) = 0$), and for all $(t,j) \in \mathrm{dom}\,\psi$ such that $j \ge N$:

$$\tau(\psi)(t,j) = \begin{pmatrix} \psi\left((j-N+1)/\Lambda, j-N\right) \\ \vdots \\ \psi\left(j/\Lambda, j-1\right) \end{pmatrix}. \tag{20}$$

Choosing $T = 1/\Lambda$ as interval of integration in (19), we obtain an estimate of ξ through a batch least-squares algorithm as follows (see Bin et al. (2019) for the same structure in the context of output regulation):

$$\begin{aligned} \xi^*(t,j) &= \underset{\theta\in\mathbb{R}}{\mathrm{argmin}}\, J_N(\theta)(t,j) \\ J_N(\theta)(t,j) &:= \left|\tau_N(X)(t,j) - \tau_N(\Phi)(t,j)\theta\right|^2. \end{aligned} \tag{21}$$

To implement the above strategy, the hybrid observer in (13) is augmented with an identifier based on the shift register variables $Y^\mu = (Y_0^\mu, \ldots, Y_N^\mu) \in \mathbb{R}^{2(N+1)}$, $Z^\mu = (Z_0^\mu, \ldots, Z_N^\mu) \in \mathbb{R}^{N+1}$, $\Phi^\mu = (\Phi_1^\mu, \ldots, \Phi_N^\mu) \in \mathbb{R}^{2N}$, related to the moving window operator as $\tau_N(\Phi) = \Phi^\mu$, $\tau_N(X) = (X_1^\mu, \ldots, X_N^\mu)$, $X_i^\mu = Z_{i-1}^\mu Y_i^\mu - Z_i^\mu Y_{i-1}^\mu$, $i \in \{1, \ldots, N\}$:

$$\begin{cases} \dot{\nu} = \mathcal{C}[\hat{\zeta}_\chi]\mathcal{J}\hat{h} \\ (\dot{Y}^\mu, \dot{Z}^\mu, \dot{\Phi}^\mu) = 0 \end{cases} \qquad \rho \in [0,1]$$

$$\begin{cases} \nu^+ = 0 \\ (Y_i^\mu)^+ = Y_{i+1}^\mu, \qquad i \in \{0,\dots,N-1\} \\ (Y_N^\mu)^+ = \mathcal{C}[\hat{\zeta}_\chi]\mathcal{J}\hat{h} \\ (Z_i^\mu)^+ = Z_{i+1}^\mu, \qquad i \in \{0,\dots,N-1\} \quad \rho = 1 \\ (Z_N^\mu)^+ = |\hat{h}| \\ (\Phi_i^\mu)^+ = \Phi_{i+1}^\mu, \qquad i \in \{1,\dots,N-1\} \\ (\Phi_N^\mu)^+ = \mathcal{J}\nu|\hat{h}|Z_N^\mu \end{cases} \tag{22}$$

$$\xi^*(t,j) = \mathcal{G}[Y^\mu, Z^\mu, \Phi^\mu](t,j) = \underset{\theta\in\mathbb{R}}{\operatorname{argmin}} J_N(\theta)(t,j),$$

where the standard Moore-Penrose pseudoinverse can be employed to compute ξ^*. The jump of $\hat{\xi}$ is then modified as a function of $\hat{\xi}$ and ξ^*. Without intending to provide a stability analysis, we propose to jump according to two criteria, i.e. the "readiness" of the shift register and the norm of the error $\hat{\xi}-\xi^*$:

$$\hat{\xi}^+ = \begin{cases} \hat{\xi} & j \le N+1 \text{ or } |\hat{\xi}-\xi^*| \le 4\sqrt{\gamma} \\ \xi^* & \text{otherwise.} \end{cases} \tag{23}$$

This way it is possible to ensure that, if the errors e_X, e_Φ are sufficiently small, the above jump improves the estimate $\hat{\xi}$, guaranteeing x_s^+ to be close to the set $W_1 \le 2$ in (9) (where $4\sqrt{\gamma}$ accounts for the worst case). Within such set, the local behavior of the attitude observer becomes dominant, ensuring a desirable behavior. Note that e_X and e_Φ can be made arbitrarily small since e_X, e_Φ vanish as $\tilde{h} \to 0$: by proper selection of k_p and k_i, $\tilde{h}$ is forced to converge during flows in an arbitrarily small ball, before any jump occurs. Finally, Figure 2 (plots (c),(f),(i),(l)) presents the simulations of the observer (13)-(22)-(23), with N as in Table 1. As expected, the proposed identifier improves the previous solution in terms of estimation speed, and a fast reduction of $\tilde{\xi}$ is obtained after a brief waiting time.

5. CONCLUSIONS

We presented a hybrid sensorless observer for PMSMs, with no a priori knowledge of the mechanical model. The rotor speed was assumed to have an unknown sign and a persistently non-zero magnitude. Here, we showed that a clock allows achieving semi-global practical stability. Motivated by the resulting convergence properties, we also proposed a speed-up strategy based on a discrete-time identifier. Future efforts will be dedicated to further investigating this identification approach.

REFERENCES

Bernard, P. and Praly, L. (2018). Convergence of gradient observer for rotor position and magnet flux estimation of permanent magnet synchronous motors. *Automatica*, 94, 88–93.

Bin, M., Bernard, P., and Marconi, L. (2019). Approximate nonlinear regulation via identification-based adaptive internal models. *arXiv preprint arXiv:1907.05050*.

Bobtsov, A.A., Pyrkin, A.A., Ortega, R., Vukosavic, S.N., Stankovic, A.M., and Panteley, E.V. (2015). A robust globally convergent position observer for the permanent magnet synchronous motor. *Automatica*, 61, 47–54.

Bosso, A., Tilli, A., and Conficoni, C. (2020). A robust sensorless controller-observer strategy for PMSMs with unknown resistance and mechanical model. *IFAC-PapersOnLine*.

Goebel, R., Sanfelice, R.G., and Teel, A.R. (2012). *Hybrid dynamical systems: modeling, stability, and robustness*. Princeton University Press, Princeton, NJ.

Hilairet, M., Auger, F., and Berthelot, E. (2009). Speed and rotor flux estimation of induction machines using a two-stage extended Kalman filter. *Automatica*, 45(1), 1819–1827.

Khalil, H.K., Strangas, E.G., and Jurkovic, S. (2009). Speed observer and reduced nonlinear model for sensorless control of induction motors. *IEEE Transactions on Control Systems Technology*, 17(4), 327–339.

Lee, H. and Lee, J. (2013). Design of iterative sliding mode observer for sensorless PMSM control. *IEEE Transactions on Control Systems Technology*, 21(4), 1394–1399.

Mahony, R., Hamel, T., and Pflimlin, J.M. (2008). Nonlinear complementary filters on the special orthogonal group. *IEEE Transactions on Automatic Control*, 53(5), 1203–1217.

Marino, R., Tomei, P., and Verrelli, C.M. (2008). An adaptive tracking control from current measurements for induction motors with uncertain load torque and rotor resistance. *Automatica*, 44(2), 2593–2599.

Mayhew, C.G., Sanfelice, R.G., and Teel, A.R. (2011). Quaternion-based hybrid control for robust global attitude tracking. *IEEE Transactions on Automatic Control*, 56(11), 2555–2566.

Montanari, M., Paresada, S., and Tilli, A. (2006). A speed-sensorless indirect field-oriented control for induction motors based on high gain speed estimation. *Automatica*, 42(10), 1637–1650.

Ortega, R., Yi, B., Nam, K., and Choi, J. (2019). A globally exponentially stable position observer for interior permanent magnet synchronous motors. *arXiv preprint arXiv:1905.00833*.

Sanfelice, R.G. and Teel, A.R. (2009). Asymptotic stability in hybrid systems via nested Matrosov functions. *IEEE Transactions on Automatic Control*, 54(7), 1569–1574.

Sanfelice, R.G. and Teel, A.R. (2011). On singular perturbations due to fast actuators in hybrid control systems. *Automatica*, 47(4), 629–701.

Sontag, E.D. (1999). Clocks and insensitivity to small measurement errors. *ESAIM: Control, Optimisation and Calculus of Variations*, 4, 537–557.

Teel, A.R., Moreau, L., and Nešić, D. (2003). A unified framework for input-to-state stability in systems with two time scales. *IEEE Transactions on Automatic Control*, 48(9), 1526–1544.

Tilli, A., Bosso, A., and Conficoni, C. (2019). Towards sensorless observers for sinusoidal electric machines with variable speed and no mechanical model: A promising approach for PMSMs. *Systems & Control Letters*, 123, 16–23.

Verrelli, C.M., Tomei, P., Lorenzani, E., Migliazza, G., and Immovilli, F. (2017). Nonlinear tracking control for sensorless permanent magnet synchronous motors with uncertainties. *Control Engineering Practice*, 60, 157–170.

Verrelli, C.M., Tomei, P., and Lorenzani, E. (2018). Persistency of excitation and position-sensorless control of permanent magnet synchronous motors. *Automatica*, 95, 328–335.

Zaltni, D., Ghanes, M., Barbot, J.P., and Abdelkrim, M.N. (2010). Synchronous motor observability study and an improved zero-speed position estimation design. In *49th IEEE Conference on Decision and Control*, 5074–5079. IEEE.